

PhenoCaB: a new phenological model based on carbon balance in boreal conifers

Fabrizio Carteni¹ , Lorena Balducci² , Alain Dupont³, Emiliano Salucci¹, Valérie Néron², Stefano Mazzoleni¹  and Annie Deslauriers² 

¹Department of Agricultural Sciences, University of Naples Federico II, Via Università 100, 80055 Portici, NA, Italy; ²Département des Sciences Fondamentales, Université du Québec à Chicoutimi, 555 boulevard de l'université, Chicoutimi, QC G7H 2B1, Canada; ³Société de protection des forêts contre les insectes et maladies, 1780, rue Semples, Québec, QC G1N 4B8, Canada

Author for correspondence:
Fabrizio Carteni
Email: fabrizio.carteni@unina.it

Received: 25 November 2022
Accepted: 13 April 2023

New Phytologist (2023)
doi: 10.1111/nph.18974

Key words: balsam fir, black spruce, bud phenology, defoliation, mechanistic model, spruce budworm.

Summary

- Traditional phenological models use chilling and thermal forcing (temperature sum or degree-days) to predict budbreak. Because of the heightening impact of climate and other related biotic or abiotic stressors, a model with greater biological support is needed to better predict budbreak.
- Here, we present an original mechanistic model based on the physiological processes taking place before and during budbreak of conifers. As a general principle, we assume that phenology is driven by the carbon status of the plant, which is closely related to environmental variables and the annual cycle of dormancy–activity. The carbon balance of a branch was modelled from autumn to winter with cold acclimation and dormancy and from winter to spring when deacclimation and growth resumption occur.
- After being calibrated in a field experiment, the model was validated across a large area (> 34 000 km²), covering multiple conifers stands in Québec (Canada) and across heated plots for the SPRUCE experiment in Minnesota (USA). The model accurately predicted the observed dates of budbreak in both Québec (± 3.98 d) and Minnesota (± 7.98 d).
- The site-independent calibration provides interesting insights on the physiological mechanisms underlying the dynamics of dormancy break and the resumption of vegetative growth in spring.

Introduction

Phenology is the study of the timing of recurrent biological events, the causes of their timing with regard to biotic and abiotic forces, and the interrelation among phases of the same or different species' (Lieth, 1974). Considering the rapid change in global climatic conditions, many studies have focussed on the effects of abiotic factors on plant phenology (Piao *et al.*, 2019). Environmental cues such as temperature and photoperiod allow plants to survive by synchronizing growth and dormancy cycles with favourable environmental conditions (Badeck *et al.*, 2004), and many mathematical models have been developed to predict phenology; however, the need for improved mechanistic models remains (Delpierre *et al.*, 2016; Piao *et al.*, 2019). Indeed, the history of modelling plant phenology extends from early statistical (empirical) approaches, which rely on the concept of 'degree-days' or 'thermal units' (Sarvas, 1974; Hänninen, 1990), to more refined process-based models (Chuine & Beaubien, 2001; Chuine, 2010). The common denominator of all such models is the direct link between environmental cues (mostly temperature and photoperiod) to the progression of each phenological phase,

that is the modelled variables are the phenological phases themselves (Caffarra *et al.*, 2011). Despite the classification of models as 'process-based', they fail to accurately represent important physiological processes such as primary growth, frost hardening and dehardening, carbon balance and bud swelling. The poor integration of the above-mentioned processes into bud phenology models may produce an overestimation of the advance of spring phenology under future climatic scenarios (Wang *et al.*, 2020).

A more process-based model would improve predictions of phenology under conditions of climate change (Tixier *et al.*, 2019; Wang *et al.*, 2020) and biotic forest perturbations, such as insect defoliation. An important example is represented by spruce budworm outbreaks in the boreal forests of Canada, as predictions suggest an increase in both duration and intensity of such events (Gray, 2008). Indeed, insect herbivory is known to alter budburst (Quiring & McKinnon, 1999; Deslauriers *et al.*, 2019). Defoliation by spruce budworm can significantly advance the budbreak of spruce and fir trees resulting in desynchronization between insects and host plants, although exposure to warmer temperatures was observed to affect budworm's larvae more than plants, thus leading to higher synchronization (Ren

et al., 2020). Current modelling approaches (for a recent review, see Piao *et al.*, 2019) mainly consider the developmental phases from autumn to spring, where chilling (cold) and forcing (warm) temperatures are required to break endodormancy and ecodormancy, respectively (Hänninen, 1990; Chuine, 2000). However, such models cannot appropriately track the complex interactions between abiotic and biotic factors that influence budbreak. As climate change alters the relationships between insects and plants (Hamann *et al.*, 2021), more physiologically based models should help to provide a better base to study any match or mismatch between plants and herbivores.

The cycle of dormancy–activity states throughout the year is mainly influenced by environmental cues regulating molecular and physiological processes. In the context of boreal conifers, temperature is recognized as the main driver of dormancy break and growth resumption (Cooke *et al.*, 2012; Singh *et al.*, 2017), whereas bud development and successive shoot elongation are associated with sugar (or carbon) coming from either reserves (i.e. hydrolysis of starch reserves (Stitt & Zeeman, 2012)) or newly produced photosynthates (i.e. solar radiation conversion into carbohydrates (Ainsworth & Bush, 2011)). Over a growing season, photosynthetic acclimation occurs for changing light (Niinemets & Valladares, 2004) and temperature conditions (Way & Sage, 2008). These seasonal changes have substantial biochemical feedbacks on plant carbon metabolism (Smith & Dukes, 2013) and nonstructural carbohydrates (NSC). The regulation of carbon metabolism over the year becomes biologically meaningful for both dormancy and growth activities (Tixier *et al.*, 2019); these processes must be studied with a holistic view, taking into account the energy needs in the form of soluble sugars and starch, to sustain bud development and primary growth.

In the context of primary growth, terminal and axillary buds represent the main functional units that produce new shoots (Damascos *et al.*, 2005) and compete for resources (Bonser & Aarssen, 2003). Resource partitioning is expected to be influenced by the number of active buds on a plant, leading to variations in phenology. In the boreal shrub *Vaccinium angustifolium*, fewer leaf buds were related to earlier budbreak, whereas fewer flowers per bud correlated with earlier flowering (Fournier *et al.*, 2020), showing how carbon partitioning among growth units can have direct effects on phenology. In this context, natural defoliation has a legacy effect that induces changes in bud and shoot–leaf allometry (Le Roncé *et al.*, 2020). Defoliation in *Pinus sylvestris* causes a reduced number of needle pairs in buds (Millard *et al.*, 2001) and fewer buds to set in autumn (Rook, 1985). In *Quercus ilex*, fewer shoots form the year following defoliation; however, a higher number of leaves are produced, indicating a more significant carbon allocation to vegetative growth (Le Roncé *et al.*, 2020). Therefore, defoliation can be used to test how carbon allocation to primary growth units (buds) affects phenology through mechanistic modelling of the plant carbon balance.

This work aimed to characterize and model bud phenology of two conifer species (black spruce and balsam fir) in different environmental conditions. Specifically, we focus on providing a physiological basis for the progression of winter and spring

nonstructural carbohydrates (NSC) following the hypothesis that the carbon balance of the tree will affect bud phenology, which will also be driven by environmental factors (temperature and solar radiation). Moreover, to further understand the impact of NSC allocation on phenology and growth, source–sink dynamics were manipulated using natural defoliation which decreases both the sources (needles) and sinks (buds). To the best of our knowledge, this model is the first attempt to fully characterize the effect of carbon allocation on the dormancy–activity cycle of conifers to predict budbreak in nondefoliated and naturally defoliated trees.

Materials and Methods

Model description

This model describes the phenology and growth dynamics of a single conifer branch as representative of the average behaviour of the whole tree. First, we assume that phenology is driven by the carbon status of the plant (Park *et al.*, 2009; Mason *et al.*, 2014; Barbier *et al.*, 2015; Deslauriers *et al.*, 2019; Tixier *et al.*, 2019), which in turn is controlled by environmental variables and the dormancy–activity status of the plant. The second main assumption of the model is represented by the response curves of the main processes of the plant to temperature (Farquhar *et al.*, 1980; Tjoelker *et al.*, 1998; Bigras *et al.*, 2001; Cooke *et al.*, 2012; Delpierre *et al.*, 2016), that is photosynthesis, cell division, tissue growth and frost hardening, driving the temporal dynamics of the simulated branch (Supporting Information Fig. S1).

Our modelled carbon balance focusses on the temporal dynamics of six state variables: soluble sugars (S), starch (St), mass of buds on the simulated branch (M), mass of the branch itself (B), growth inhibitors that regulate branch growth (I) and the plant's carbon reserves outside the branch (C) (Fig. 1). The mass of needles on the branch (N) is not represented as a state variable, but it is assumed to be a fixed proportion (that can be reduced by defoliation, see next section) of the branch mass B . First, soluble sugars are produced by net photosynthesis (PS) which can be, according to the season, locally accumulated as starch (St) when there are no active sinks ($ACCUMULATION$), translocated to other organs of the plant to support the primary and secondary growth of roots and the stem and replenish the plant reserves ($TRANSLOCATION$) or used in the spring for the resumption of meristematic activity until budbreak ($SWELLING$) and subsequent growth of the branch and needles ($GROWTH$). When the quantity of soluble sugars is insufficient to support the sink demands, mobilization of local ($MOBILIZATION$) and plant ($MOBILIZATION_{stock}$) starch compensates the carbon demand. Moreover, from autumn to winter, lowering temperatures induce cold acclimation where soluble sugars are accumulated in the branches to increase frost resistance at the expense of starch reserves accumulated both in the same branch ($FROST HARDENING_1$) or the rest of the plant ($FROST HARDENING_2$). During the deacclimation phase, when the temperature increases from winter to spring, the opposite process occurs where soluble sugars are reconverted to starch both locally ($FROST DEHARDENING_1$) and in other organs ($FROST DEHARDENING_2$).

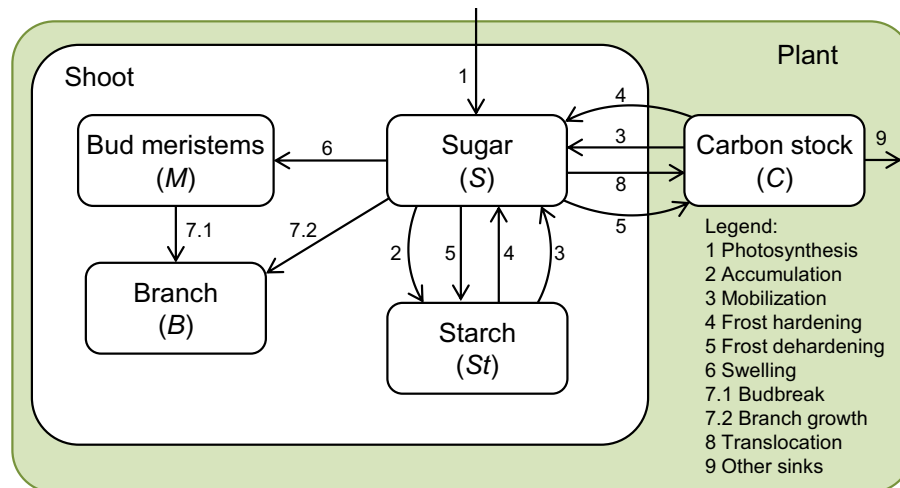


Fig. 1 Schematic representation of model variables and main processes used to predict budbreak. 1, Photosynthesis: photosynthesis in the leaves (shoots), as a source of carbon; 2, Accumulation: passive process of carbon allocation to starch reserves when sugar supply exceeds demand; 3, Mobilization: active process of starch breakdown; 4, Frost hardening: sugars accumulate in leaves during cold acclimation; 5, Frost dehardening: conversion of extra sugars into starch during the spring deacclimation; 6, Swelling: sugar allocation during the process of bud swelling; 7.1, Budbreak: opening of the bud and beginning of branch growth; 7.2, Branch growth: sugar consumption for branch growth; 8, Translocation: sugar translocation (phloem loading) to other organs; 9, Other sinks: relevant processes of other plant organs that require carbon (e.g. roots primary growth and secondary growth).

A complete description of the mathematical equations representing the above-mentioned processes and related biological assumptions is provided in Methods S1.

Model inputs, outputs and numerical simulations

The presented model runs at daily scale, and the climatic inputs considered were average air temperature (T) and photosynthetically active radiation (PAR). The only exception is the process of net photosynthesis (PS , Eqn 1 in Methods S1), which is computed using hourly inputs (both air temperature and PAR) and then aggregated to provide the daily net amount of photosynthates produced. In all other equations, daily average air temperature (T) is used to compute the functional responses (RC) of the different processes as shown in Table S1.

To assess and predict the effect of defoliation by spruce budworm, we used two inputs for the model. First, the percentage of needles destroyed in the previous season (i.e. defoliation intensity of the previous year, defined as def_{past} in Table S2) influences the calculation of needle dry weight (N , Table S1) and the intensity of self-shading and other compensation phenomena related to photosynthesis (Iqbal *et al.*, 2012). Previous-year defoliation influences the initial mass of needles on the plant, thus influencing the photosynthetic capacity (Battaglia *et al.*, 2011). Second, the intensity of current year defoliation (defined as def in Table S2) is assumed to influence the number of undamaged buds at the beginning of the growing season in a nonlinear manner (variable d in Table S1). At low levels of defoliation, the number of buds is not influenced, as compensation can be observed with the formation of epicormic buds (Piene, 1989). As defoliation severity increases, there are fewer buds, influencing carbon allocation and thus phenology at growth resumption (Fournier *et al.*,

2020; Le Roncé *et al.*, 2020). All the above-mentioned data inputs and their units are listed in Table S2.

To further explore the model behaviour and understand its response to both abiotic and biotic factors, we performed a set of theoretical simulations with different temperature and defoliation regimes. The shift in budbreak (in days) was recorded in relation to variable annual mean temperatures (between -2°C and $+2^{\circ}\text{C}$) and level of defoliation (between 0% and 100%). Therefore, simulations of a *virtual* plant were performed using a theoretical temperature curve calculated as a sinusoidal function to allow the easy modulation of the mean annual temperature of each climatic scenario as follows:

$$T = T_{\text{mean}} + \text{ampl} \cdot \cos\left(\frac{2\pi}{p} \cdot t\right) \quad \text{Eqn 1}$$

where T is the calculated daily temperature ($^{\circ}\text{C}$), T_{mean} is the climatic scenario parameter changing between -2°C and $+2^{\circ}\text{C}$, ampl is the curve amplitude, which was set to 20°C , p is the period of the function, that is the number of days in a year ($p = 365$), and t is the time-independent variable that ranges from 1 to 396, that is the number of days of a simulation.

The main model outputs were branch mass (g, dry weight), concentration of soluble sugars and starch (expressed in mg per g of branch dry weight) and predicted day of budbreak expressed as day of the year (DOY). As already described in the previous section, the budbreak date was computed by the model algorithm as the day in which the buds' mass (M) reached a threshold value equal to two times their initial mass (see SW_V formulation in Table S1).

To capture the dynamics of cold acclimation and dormancy, followed by the resumption of growth until the cessation of the vegetative season, each simulation run began on 1 August of one

year until 31 August of the next year. The equations were numerically integrated using MATLAB R2020b (The MathWorks, Natick, MA, USA) with a variable order solver (ode15s) based on numerical differentiation formulas, which are particularly efficient with stiff problems (Shampine & Reichelt, 1997).

Model calibration and validation

The presented model was calibrated and then validated separately on four datasets, the first two for calibration and the second two for validation. Calibrated parameters are reported in Table S3 and details of the experimental plots, data collection and calibration procedure are described in Methods S1; Tables S4, S5; Figs S2 and S3.

The first calibration dataset (Deslauriers *et al.*, 2019) was obtained from a glasshouse experiment performed between 2015 and 2016 and included 4-yr-old saplings of white spruce (*Picea glauca* (Moench) Voss), black spruce (*Picea mariana* B.S.P. (Mill.)) and balsam fir (*Abies balsamea* (L.) Miller).

The second calibration dataset (Huang *et al.*, 2014; Antonucci *et al.*, 2015) came from the long-term field monitoring experiment of balsam fir and black spruce adult trees from 2011 to 2019 in Gaspard (Monts-Valin National Park, Canada) where natural defoliation by spruce budworm began in 2016 (Table S4).

The third dataset (validation) comprised 20 experimental plots in Québec (Canada) that were provided by the monitoring programme of SOPFIM, La Société de Protection des Forêts contre les Insectes et les Maladies. The sites were spread across different locations and elevations within the eastern boreal forests of Québec (Canada). Bud phenology was recorded between 2010 and 2021 for balsam fir and 2015 and 2021 for black spruce (Table S4). Because weather stations were not available at each site, the model simulations were performed using climate data (temperature and solar radiation) extracted from the software BIOSIM v.11 (Régnière *et al.*, 2017) as explained in Methods S1. The use of interpolated climate inputs (BIOSIM data) did not significantly hinder model predictions at the long-term experimental plot ($R^2 = 0.95$; Fig. S4); BIOSIM climate data were then used to simulate budbreak for the 20 SOPFIM sites.

The fourth dataset (validation) comes from the long-term observations of black spruce collected from 2016 to 2020 by Spruce and Peatland Responses Under Changing Environments (SPRUCE) experiment located within in the USDA Forest Service Marcell Experimental Forest in Minnesota, USA (Hanson *et al.*, 2017; Richardson *et al.*, 2018; Schädel *et al.*, 2019, 2020, 2021). Statistical analyses (two-way ANOVA with DOY as dependent variable and CO₂ and temperature treatments as independent variables and a GLM with DOY as response variable and CO₂ and temperature as categorical predictors) to test whether treatments with elevated ambient CO₂ influenced spring phenology were performed. Only controls and experiments with temperature treatments were considered in the presented work.

For all datasets, the stages of bud phenology were analysed as a qualitative variable and expressed as their frequency observed over each sampling day, expressed as DOY. We applied an

ordinal regression model for predicting the progression of stages between years and sites for each species. We used the DOY at which there is a 50% of probability of transition from the last two stages, that is the transition to open buds. Details of the statistical procedure are reported in Methods S1.

Moreover, to set a benchmark to compare part of the predictions provided by the presented model (i.e. spring phenology), a standard Growing Degree Days (GDD) forcing model was also calibrated and validated for black spruce and balsam fir using the same datasets described previously. In particular, the second (long-term field experiment in Gaspard, Canada) and the third (monitoring programme of SOPFIM in Quebec, Canada) datasets were merged and divided in half to be used for calibration and validation of the GDD model. Additionally, the fourth dataset (SPRUCE experiment in Minnesota, USA) was used as further validation. Details of the used forcing model and the calibration/validation procedures are described in Methods S2.

Results

Model calibration: dynamics and defoliation effect in the glasshouse experiment

The presented model has been first calibrated on both control and defoliated saplings grown in a glasshouse. The simulation shown in Fig. 2 has the purpose to illustrate the model behaviour, including the temporal dynamics across the annual cycle of buds, branch and needle mass, total soluble sugars and starch. As expected for the calibration procedure, model simulations agreed well with measured experimental data in both controls and defoliated plants (Fig. 2).

To explain the model functioning and rationale, we describe below the behaviour of *P. mariana* saplings (Fig. 2) as representative of all species (Fig. S5). The simulation starts from the beginning of August 2015 when the simulated sapling had already ended the vegetative cycle, thus assuming no variation in bud, branch and needle mass during this period (Fig. 2). The concentration of sugars in the twig remained almost constant until the end of November at $c. 19 \text{ mg g}^{-1}$ for control plants and $c. 14 \text{ mg g}^{-1}$ for defoliated plants, whereas starch slowly accumulated to 23 mg g^{-1} in controls and 2 mg g^{-1} in defoliated treatments because photosynthesis was still active, and primary growth had ended. Until the end of winter, soluble sugars in the branch progressively increased, peaking at a concentration of $c. 88 \text{ mg g}^{-1}$ around the end of April, whereas in the same period starch concentrations were near zero for both control and defoliated plants.

Starting from May 2016, air temperature started to rise above freezing, lowering the process of frost hardening, thus leading to cold deacclimation. From this moment, sugar accumulated for frost hardening dropped rapidly to 17.5 mg g^{-1} in both treatments. Part of the soluble sugars deriving from cold deacclimation were locally reaccumulated as starch in the branch up to a concentration of 35.2 mg g^{-1} in controls and 19.9 mg g^{-1} in defoliated plants. Another portion was translocated to the rest of the plant to feed other sinks (i.e. root reactivation). During May, increasing temperatures reactivated the meristems within the

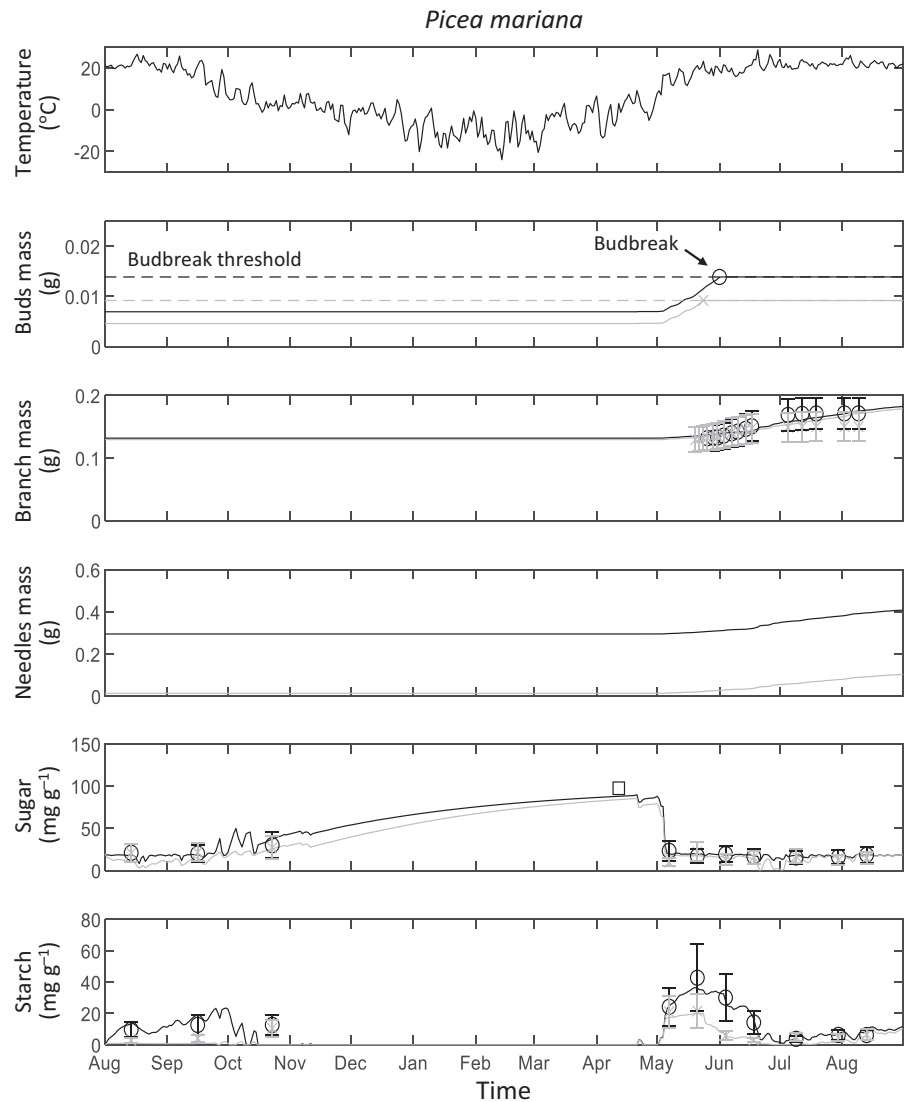


Fig. 2 Model simulations including nondefoliated control (black lines) and defoliated saplings (grey lines) of *Picea mariana* grown during the glasshouse experiment. The simulations (continuous lines) are compared with experimental data across an annual cycle spanning from August 2015 to August 2016 for the nondefoliated control (open circles) and defoliated plants (crosses) \pm SD. The simulated variables include bud mass (g) with the budbreak threshold (dashed line), branch mass of developing branch (wood) and needles (g), total sugar and starch concentration within the branch and buds (mg g^{-1} DW). The square in the sugar plot represents unpublished data.

buds. Bud mass steadily grew until they reached the set threshold, leading to budbreak on 1 June in controls and 8 d earlier (24 May) in defoliated plants (Fig. 2, bud mass).

The simulated number of buds (expressed as bud mass in Fig. 2) at the beginning of the model annual cycle was lower in defoliated plants (0.0046 g) than control plants (0.0069 g) because of the direct effect of spruce budworm activity (see ‘Model description’ in the Materials and Methods section for details). Moreover, owing to the lower needle mass (0.015 g in defoliated vs 0.295 g in control plants) at the beginning of the model annual cycle (Fig. 2, needle mass), photosynthesis produced less sucrose, resulting in lower accumulation of starch during primary growth between the end of June and beginning of July. Following budbreak, branch growth proceeded, resulting in both lengthening of the shoot and production of new needles until the beginning of July, with no marked difference between treatments (Fig. 2, branch mass). Branch mass increased by 0.05 g, whereas needle mass increased by 0.10 g, although needle mass started from 0.295 g in controls and 0.015 g in defoliated plants.

With the onset of twig growth, we observed a marked decrease in starch (to a minimum concentration of 0.9 mg g^{-1} in controls and 0.3 mg g^{-1} in defoliated plants). This starch was converted to simple sugars and used to support the carbon needs of newly produced biomass (Fig. 2, starch). When primary growth stopped by the end of July, the concentration of soluble sugars stabilized at $c. 18 \text{ mg g}^{-1}$ for both treatments, whereas starch concentrations were $c. 11.7$ and 10.3 mg g^{-1} for control and defoliated plants, respectively (Fig. 2, sugar and starch plots).

Model calibration of adult trees in the long-term field experimental plot

The model was further calibrated for balsam fir and black spruce adult trees within the long-term experimental plot in Gaspard (plot SLSJ2, Table S4). In general, the calibrated parameters (Table S3) allowed the model to correctly reproduce observed dates of budbreak for both undefoliated (2011–2015) and defoliated trees (2016–2019) with an $R^2 = 0.93$ (Fig. 3), and

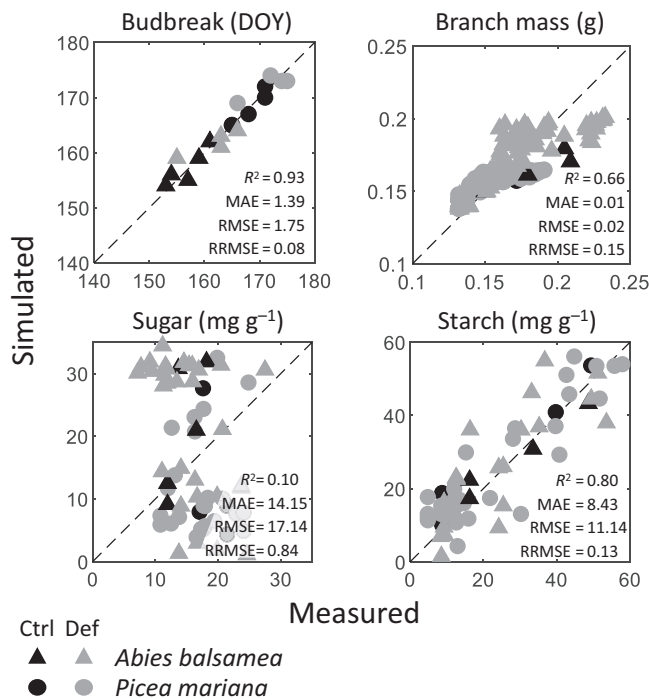


Fig. 3 Measured vs simulated variables for the model calibration of the long-term field experiments for both the nondefoliated control (Ctrl, black symbols) and defoliated (Def, grey symbols) *Abies balsamea* and *Picea mariana* plants. DOY, day of the year; MAE, mean absolute error; RMSE, root mean square error; RRMSE, relative RMSE.

differences in phenology between fir (mean DOY of 158.0) and spruce (mean DOY of 168.7), with an earlier bud opening in fir of *c.* 10 d (Fig. 4). We also observed similar variations in the date of bud opening from year to year for both species (Fig. 4) and, in both cases, the inclusion of the effect of defoliation improved the simulations of budbreak (Fig. 4), with a maximum divergence between simulations and observation of 3 d. Regarding the other simulated variables, the simulated branch mass ($R^2 = 0.66$) and starch concentration in the branch ($R^2 = 0.80$) agreed well with the measured data (Fig. 3). On the contrary, the model was

unable to reproduce the measured variations of soluble sugars in the branch ($R^2 = 0.10$).

Model validation at a larger scale

To test the model's predictive capability, we validated the model using two different datasets of black spruce phenology and one for balsam fir. The selected sites are in different biogeographical areas, the first one in the eastern Canadian boreal shield and Atlantic Maritime ecozones of Québec, and the second is at the southern margin of the boreal peatland forest located in the upper Midwest of USA (Minnesota; Fig. 5).

In relation to the data collected from 20 sites in Québec, the model produced accurate predictions for both fir and spruce with an overall mean absolute error of ± 3.98 d ($R^2 = 0.62$; inset in Fig. 5b). In general, mature balsam fir showed an earlier budbreak than black spruce, and the mean absolute error for balsam fir was slightly lower (± 3.9 d) than black spruce (± 4.2 d).

The second validation test used the dataset from the SPRUCE experimental chambers in Minnesota. Several plots of black spruce with different temperature treatments were selected (ambient temperature, control chamber and chambers with $+2.25^\circ\text{C}$, $+4.5^\circ\text{C}$, $+6.75^\circ\text{C}$ and $+9.0^\circ\text{C}$). The model performed well ($R^2 = 0.79$) with an overall mean absolute error of 7.98 d (Fig. 5a). As expected, the simulated budbreak was progressively anticipated with increasing temperatures with an average difference between the trees outside the chambers and the $+9.0^\circ\text{C}$ treatment of almost 7 wk (48.2 d) with an average advance in phenology of $5.4 \text{ d } ^\circ\text{C}^{-1}$.

To understand the predictive capability of the presented model in comparison with classical models based on thermal sums, we calibrated and validated a GDD forcing model whose results are presented in Fig. S6. For the first validation test (randomly selected half of the sites of the Monts-Valin National Park plus the SOPFIM datasets), the GDD model performed similarly to PhenoCaB, with an overall mean absolute error of ± 3.2 d ($R^2 = 0.78$). The second validation test using the SPRUCE experiment

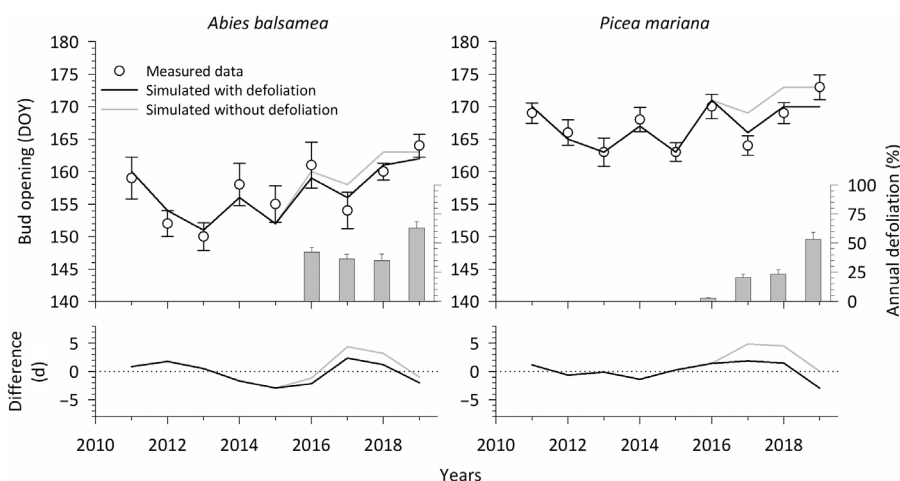


Fig. 4 Budbreak date observed for balsam fir (left) and black spruce (right) trees at the long-term field experimental site in Gaspard, Québec (SLSJ2) from 2011 to 2019. Shoot defoliation (%), and SE) occurred from 2016 to 2019 (grey histogram) after the first presence of dead butterflies was detected in August 2015. Phenological observations (circles \pm SD) are compared with simulations performed with the model including (black lines) or not (grey lines) the effect of defoliation. Differences (in days) between observed and simulated phenology are illustrated in the bottom plots. DOY, day of the year.

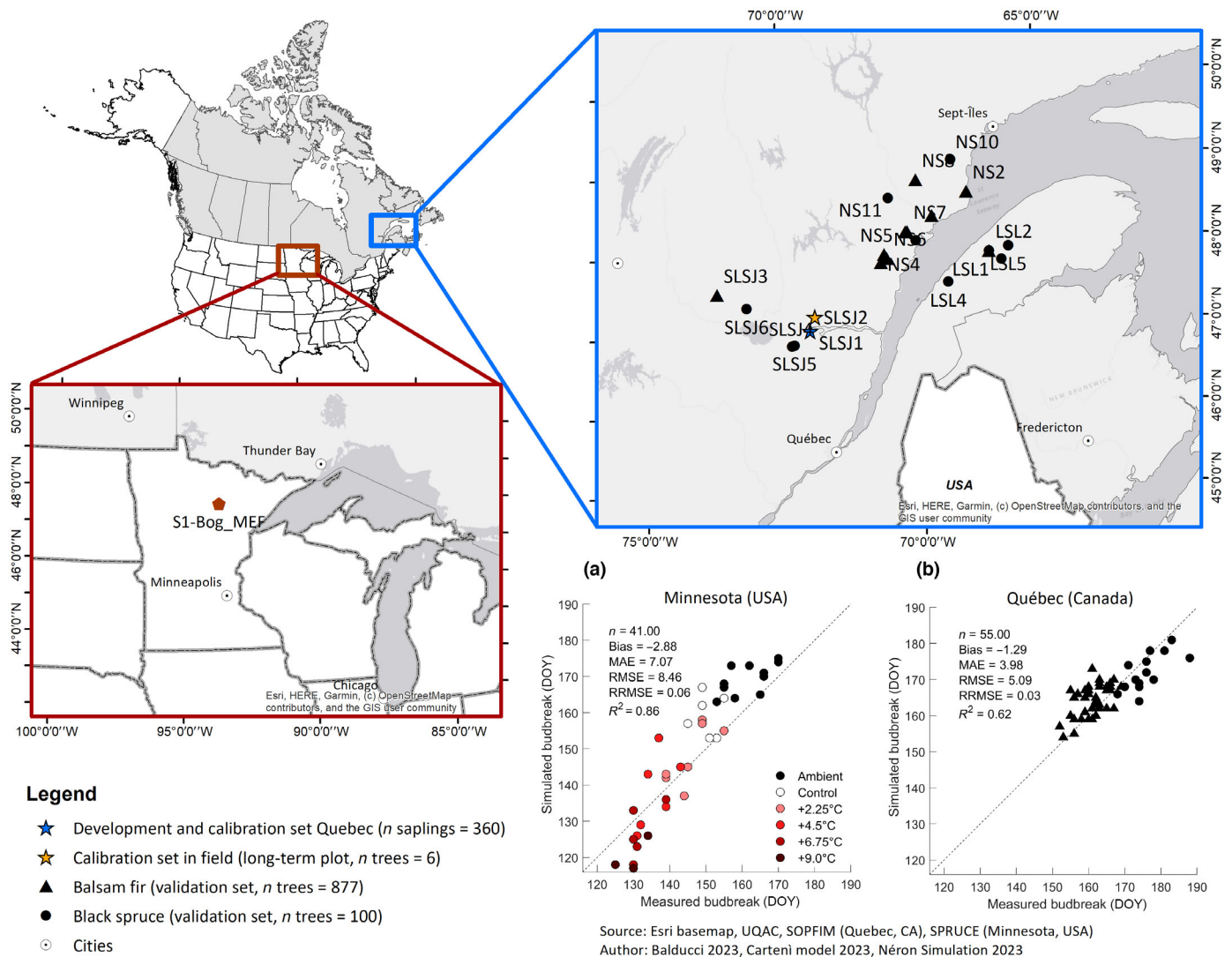


Fig. 5 Location in Québec (Canada) and in Minnesota (USA) of the experimental plots used for model development, calibration and validation. The map shows the glasshouse experimental site (blue star), the long-term experimental site (yellow star), the field validation plots for balsam fir (black triangles) and black spruce (black circles) in Québec and a second independent validation site for black spruce in the Minnesota (dark red pentagon). The insets on the bottom right corner show the model predictive performance in the validation sets (a) SPRUCE Marcel Experiment Forest in Minnesota (USA) under changing temperature and (b) SOPFIM under ambient air temperature in Québec (Canada). See Supporting Information Table S4 for the plot characteristics. DOY, day of the year; MAE, mean absolute error; RMSE, root mean square error; RRMSE, relative RMSE; SOPFIM, La Société de Protection des Forêts contre les Insectes et les Maladies; SPRUCE, Spruce and Peatland Responses Under Changing Environment.

dataset resulted, among all temperature treatments, in a mean absolute error of ± 7.05 d with a $R^2 = 0.84$ (Fig. S6).

Theoretical simulations of responses to abiotic and biotic factors

We ran theoretical simulations to investigate the response (in terms of days of shift in budbreak) of virtual plants to variations in annual mean temperature (between -2°C and $+2^\circ\text{C}$) and different levels of defoliation (between 0% and 100%). In the model response to the abiotic and biotic factors, we observed that, for both species, budbreak responded strongly (and mostly linearly) to variations in mean annual temperature, showing that this process is highly sensitive to temperature (Fig. 6). In the absence of defoliation, an increase in temperature of 2°C

produced an earlier budbreak of 8 d for both species, whereas a decrease of 2°C induced a delay of 8 d for *P. mariana* and 9 d for *A. balsamea*. In general, these simulations showed an advance of $c. 4 \text{ d } ^\circ\text{C}^{-1}$ of temperature difference. On the contrary, defoliation had less of an effect on budbreak shift with some differences for the two simulated species. For *P. mariana*, budbreak occurred 2 d earlier with a defoliation intensity $\geq 20\%$, whereas *A. balsamea* exhibited the same shift of budbreak with defoliation $\geq 40\%$ (Fig. 6).

Effect of elevated ambient CO_2 treatments on spring phenology

To test whether elevated CO_2 treatments influence spring phenology, we analysed the datasets of the SPRUCE experimental

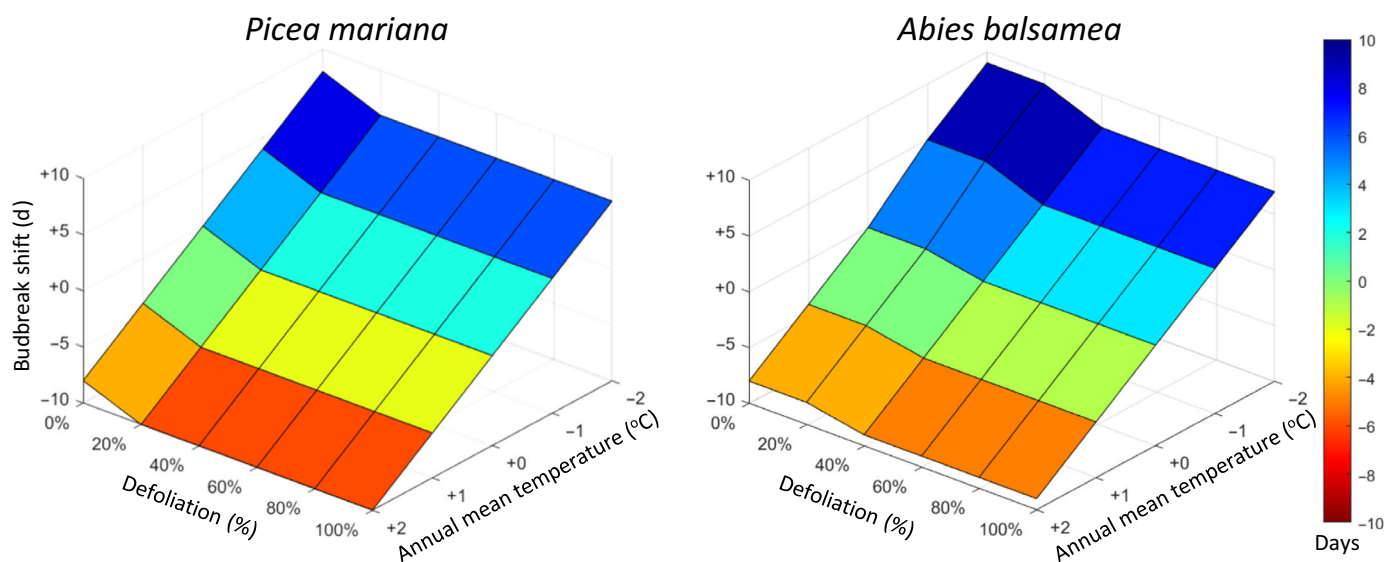


Fig. 6 Surface plots showing the variation (in days) of the simulated budbreak date in relation to changes in annual mean temperature and defoliation intensity for black spruce (left) and balsam fir (right).

chambers. First, we plotted all the available observations of budbreak dates in the different temperature (+0°C, +2.25°C, +4.5°C, +6.75°C and +9°C) and CO₂ (+0 and +500 ppm) treatments (Fig. 7). As shown in Table S6, results of the two-way ANOVA performed on the dataset confirms a highly significant effect of the temperature treatments ($F = 30.7$, $P < 0.001$) while revealing no significant effect of the elevated CO₂ treatment ($F = 0.6$, $P = 0.43$). To further test the effect of temperature and

elevated CO₂ as best predictor of DOY, we also built a GLM with DOY as response variable and CO₂ and temperature treatments as categorical predictors (Table S7). The GLM results confirm a significant negative effect of high-temperature treatments (+4.5°C, +6.75°C and +9°C) on budbreak DOY ($P < 0.001$), while no effect of elevated CO₂ and no effect of the interactions of treatments except for the combination between elevated CO₂ and the +9°C temperature ($P = 0.0075$).

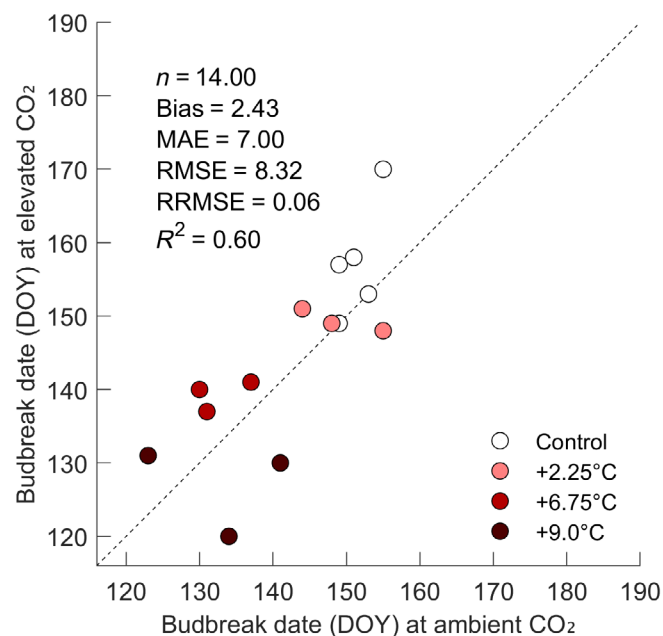


Fig. 7 Analysis of the effect of elevated CO₂ on budbreak dates of black spruce at different temperature levels in the SPRUCE Marcel Experiment Forest in Minnesota (USA). DOY, day of the year; MAE, mean absolute error; RMSE, root mean square error; RRMSE, relative RMSE, SPRUCE, Spruce and Peatland Responses Under Changing Environment.

Discussion

Carbon balance-based approach to simulating budbreak and primary growth

The presented model PhenoCaB simulates the main carbon fluxes of the plant and the responses of these fluxes to the environment, with particular focus on the translocation of carbon within the plant (e.g. frost hardening and dehardening over winter), the production of soluble sugars by photosynthesis and their interconversion with starch, and meristematic activity with the production of new shoots and needles. With this approach, phenological phases are viewed simply as emergent properties of the complex interactions of the plant's physiological processes that lead to events such as budbreak, which is the first manifestation of the resumption of vegetative growth. Confirming our first hypothesis, the branch carbon balance, driven by the dormancy-activity state and environmental factors (temperature and solar radiation), proved as a relevant mechanism driving spring phenology. The acclimation phase during winter dormancy, that is the accumulation of soluble sugars within the buds, provides readily available substrates for the following spring deacclimation, driving important physiological processes that influence the resumption of meristematic activity and thus spring phenology. This scenario highlights the importance to these trees of finely tuning the carbon allocation across the annual cycle (Tixier

et al., 2019). The model simulated the continuous process of bud mass increase by cell division and differentiation of leaves during swelling (González-González *et al.*, 2013), which is visually observed in the phases leading to budbreak (Rossi & Isabel, 2017). The validation performed in 21 sites across North America demonstrated the model's predictive capability, accurately estimating observed phenology at large scale (> 34 000 km²) with a mean absolute error of 3.98 d for Québec and 7.98 d for Minnesota, highlighting also the modelling approach potential to simulate climate warming scenarios.

Our model correctly simulated the pathway of conversion from starch to sugar in fall and the opposite process in spring (Tixier *et al.*, 2019; Deslauriers *et al.*, 2021). During autumn, when decreasing photoperiod and temperature induce both endo- and ecodormancy (Singh *et al.*, 2017), the exposure to chilling promotes sugar accumulation in all living cells, the sugars being mainly sucrose and some other oligosaccharides (Meng *et al.*, 2015; Taïbi *et al.*, 2018; Deslauriers *et al.*, 2021). Our simulated starch and sugar patterns during winter agree with the literature (Schaberg *et al.*, 2000), where the accumulated sugar can increase to > 25 times the concentrations observed during summer (Strimbeck *et al.*, 2015). During late winter and early spring, cold hardiness in conifers is rapidly lost (Man *et al.*, 2017) with temperature being the primary factor driving this process (Bigras *et al.*, 2001). As cold hardiness decreases, a high sugar content triggers dehardening with starch formation (Lunn *et al.*, 2006). Starch is then hydrolysed when carbon consumption for budburst and primary growth increases (Decourteix *et al.*, 2008; Klein *et al.*, 2016). In all simulations, measured starch concentrations agreed well with the simulated data (Fig. 3). Differently, after parameter calibration the model was not able to properly reproduce the observed patterns of soluble sugars (Fig. 3), most probably because of the small scale of variations observed during summer (Deslauriers *et al.*, 2014). As previously observed at larger temporal scales, the major differences of sugar concentrations in buds are observed between the spring–summer and autumn–winter periods increasing from *c.* 50 up to 300 mg g⁻¹ (Svobodová *et al.*, 2000). However, the overall inter-seasonal patterns of soluble sugars simulated here (Fig. 2) are consistent with published data (Schaberg *et al.*, 2000; Schoonmaker *et al.*, 2021).

Effect of resource partitioning

Our model explicitly considers buds as the main functional units competing for carbon resources. Sucrose allocation is fundamental for sink development (Koch, 2004), and primary meristems are the source of signal perception for growth resumption responding to sugars (Park *et al.*, 2009; Barbier *et al.*, 2015) and gene expression of growth regulators (Cooke *et al.*, 2012). Interestingly, a recent work by Zani *et al.* (2020) analysing the combined effect of source–sink dynamics and environmental factors on autumn phenology of temperate deciduous tree species found that sink limitation plays a relevant role in regulating the length of the growing season, suggesting that carbon allocation within the plant is at least as important as environmental factors for the modulation of phenological cycles.

The presented work considered the dynamics of a single average shoot as representative of the whole plant, a simplification needed to simulate the growth and shoot dynamics at stand level. Both budbreak and shoot growth are known to vary within the crown and in relation to tree height (Seiwa, 1999; Woodruff & Meinzer, 2011). Such effects are most probably caused by the independent response of each branch to its specific microclimatic conditions (Vitasse *et al.*, 2021). In 60-m-tall Douglas fir, shoot length was found to decrease linearly with height, while NSC followed the opposite pattern (Woodruff & Meinzer, 2011). In smaller white spruce (*c.* 8 m tall), no height pattern was found in NSC concentration (Schoonmaker *et al.*, 2021). Our modelling approach could indeed be extended to consider the behaviour of single branches in relation to tree height and their specific position within the crown, while keeping track of the total NSC pool of the plant (Schoonmaker *et al.*, 2021).

The relevance of source–sink dynamics was further highlighted by the simulation of defoliated plants that, having fewer sinks, reduce interbuds competition. Because the mass of buds was lower in defoliated plants, although the amount of stored carbon remained considerable, the amount of sugar allocated per unit of bud mass was slightly higher in defoliated plants than in controls resulting in advanced bud opening. The modelled bud phenology of defoliated trees is consistent with current knowledge on the effects of spruce budworm on boreal species. In fact, earlier budbreak was observed in different conifers (Deslauriers *et al.*, 2019) and poplar (Park *et al.*, 2009) by manipulating the source–sink balance or the expression of sucrose phosphate synthase, respectively. In natural stands affected by spruce budworm, other internal or external factors might also influence the resource partitioning to primary growth and thus the timing of bud phenology. During insect attack, carbon could also be invested into reproduction (Lauder *et al.*, 2019; Bouchard & Pernot, 2021) or the production of defence components (Celedon & Bohlmann, 2019) although for the latest, no trade-off was found between NSC and terpene production, both decreasing under higher defoliation in balsam fir (Deslauriers *et al.*, 2015). Important nutrient changes in soil and leaves were also reported during spruce budworm outbreaks (De Grandpré *et al.*, 2022), with potential direct effects on stomatal movement and photosynthesis via potassium decrease (Wang & Wu, 2017) or indirect effects on phenology via nitrogen increase (De Barba *et al.*, 2016).

Model responses to combined abiotic and biotic factors

Bud phenology is strongly influenced by temperature. A phenological data network in Europe and North America confirms that plant phenology is highly responsive to increasing temperatures (Menzel *et al.*, 2006; Cook *et al.*, 2012). Indeed, an increase in monthly maximum temperature of 1°C between 1982 and 2011 advanced spring phenology by 3 d in the Northern Hemisphere (Piao *et al.*, 2015). A +2°C experimental warming advanced spring phenology by an average *c.* 2 d in *A. balsamea* and *P. mariana* (Bellemin-Noël *et al.*, 2021), and natural black spruce stands experienced earlier budbreak up to 3 d for each 1°C increase (Pureswaran *et al.*, 2019). A stronger effect was observed for

P. mariana between 2016 and 2020 in the SPRUCE experiment in Minnesota, USA (Hanson *et al.*, 2017; Richardson *et al.*, 2018; Schädel *et al.*, 2019, 2020, 2021), where an advance of 5.4 d °C⁻¹ of temperature increase was observed and correctly simulated in the validation tests (Fig. 5).

Increased temperatures cause variations in leaf traits, induce strong photosynthetic thermal acclimation (Way & Sage, 2008) and alter the carbon balance, affecting bud phenology. A 2°C rise can result in accelerating the exit of buds from winter dormancy, reduce cold hardiness coupled with a parallel increase in starch concentration (Adams *et al.*, 2013) and increase photosynthesis (Reich *et al.*, 2018). Moreover, considering the legacy effects of the previous autumn and winter temperature on phenology and shoot growth (Beil *et al.*, 2021), knowledge about the seasonal changes in NSC pools and how they are related to phenology might help in disentangling contrasting effects of specific warmer or colder periods during the dormancy–growth cycle. Our theoretical model simulations detected these opposite effects of colder and warmer temperatures on budbreak. An increase of 2°C promoted an earlier budbreak of 8 d for both species, whereas temperatures 2°C colder delayed budbreak by 8 d for *P. mariana* and 9 d for *A. balsamea*. Our results agree with phenological observations of extended time series across the Northern Hemisphere, highlighting an asymmetric effect of warming and cooling temperatures on budbreak (Liu *et al.*, 2016; Signarbieux *et al.*, 2017). These findings emphasize the importance of a solid understanding of the effect of interannual variations in temperature on the relevant physiological processes. Here, we provide more biologically realistic representations of the effects of low temperatures during dormancy (i.e. chilling) and warm spring temperatures (i.e. forcing), linking their effect to starch degradation–synthesis rates (Zwieniecki *et al.*, 2015).

Considering the combination of defoliation and temperature scenarios, we observed that *P. mariana* was more sensitive than *A. balsamea* in terms of species' immediate response to defoliation levels over 20%. *Abies balsamea*, however, exhibited a 2-d advance in budbreak only when defoliations increased to 40%; this earlier budbreak increased to 3 d when the temperatures were colder (−2°C scenario). Similarly, a study of black spruce showed this host tree to be highly responsive to warmer temperatures that counteracted an advance in the phenology of host trees subjected to defoliation (Ren *et al.*, 2020).

Comparison with other modelling approaches

Compared with traditional phenological models (Cannell & Smith, 1983; Hänninen, 1990; Chuine, 2000), PhenoCaB is more complex in terms of number of equations and parameters because of the necessity to reproduce all relevant physiological and growth processes involved in the plant dormancy–activity cycle. Obviously, this complexity invokes some costs, mostly in terms of data requirements for a proper calibration and computational performance that renders simulation and calibration procedures more time-consuming. However, we believe that the conceptual advantages and power of a more realistic representation of both abiotic and biotic effects on phenology justify such

costs. A physiological process-based model requiring calibration at the species level (site independent) is clearly robust in its potential application and capability of simulating phenology and other NSC-dependent processes such as frost resistance and primary growth under dynamic environmental conditions.

In principle, one of the main advantages of the presented approach is the site-independent calibration, solving one of the main limitations of traditional phenological models (Basler, 2016). To test this advantage, we validated the model on a much wider spatial scale than that for the calibration sites (Fig. 5). At this larger scale, our budbreak simulation results produced a mean absolute error of 3.9 d for *A. balsamea* and 4.2 d for *P. mariana* in Québec (Canada) and 7.98 d in Minnesota (USA) for *P. mariana*.

We also applied a classical Growing Degree Days model as a benchmark for the performance of the phenological predictions. Interestingly, the GDD model tests yielded similar results compared with PhenoCaB (Fig. S6), confirming that temperature is the main driver of spring phenology in the studied sites. These results probably come from the low heterogeneity of environmental conditions that characterize the studied portion of North America. Even providing similar predictions, our results bear important consequences for the study and understanding of the internal processes driving winter and spring phenology, providing a potential physiological explanation for the concepts of chilling and forcing which may drive further investigations on the direct involvement of carbohydrates metabolism and their dynamics on the internal plant clocks.

Basler (2016) tested several published traditional models of leaf unfolding by running various combinations of photoperiod and chilling and forcing temperatures using a large European dataset of hundreds of sites covering over 40 yr and six species. When each model was calibrated for all sites at the same time, the overall error was *c.* 7–9 d, whereas the error decreased to 4–5 d when the models were separately calibrated for each site. Piao *et al.* (2019) reported similar results in terms of performance in a review of models. Comparatively, our model produced similar results although after calibration on a 9-yr series at a single site.

Several factors were not considered in the present formulation of the model that may have an impact on carbon allocation and phenology. For instance, the effects of water or nutrient availability could become relevant, especially for plants in environments characterized by limited rainfall regimes or poor soil fertility. Intraseasonal NSC variations during spring and summer are indeed also influenced by the water status of the trees (Deslauriers *et al.*, 2014). Another example could be the effect of increased atmospheric CO₂ concentrations where contrasting effects have been reported for conifer species. Most authors report no effect of elevated CO₂ on spring phenology of black spruce (Johnsen & Seiler, 1996; Bigras & Bertrand, 2006), Norway spruce (Laitat *et al.*, 1994; Murray & Ceulemans, 1998), Douglas fir (Guak *et al.*, 1998), Engelmann spruce (Chomba *et al.*, 1993), whereas elevated CO₂ resulted in advanced budbreak in Scots pine (Repo *et al.*, 1996; Jach & Ceulemans, 1999) and delayed budbreak in Sitka spruce (Murray *et al.*, 1994). The analysis of the SPRUCE

experimental dataset presented here also revealed no significant effect of the elevated CO₂ treatment on spring phenology of black spruce. The most probable cause for the lack of effects of elevated CO₂ on spring phenology of many boreal conifers may lie in the specific adaptations of photosynthesis. For instance, Way & Sage (2008) studied the response of photosynthesis of black spruce to CO₂ at different temperature regimes and found that net CO₂ assimilation is mostly saturated at current levels of CO₂. Further experimental work should focus on the combined observations of phenology, branch growth and NSC dynamics at different CO₂ levels in order to extend the current formulation of the PhenoCaB model and provide more insights on the contrasting observations reported for several conifer species.

Conclusions

The presented model was able to reproduce the general trends of the annual dynamics of both internal (soluble sugars and starch) and external (branch biomass) variables that drive phenology and was successfully tested at different scales while also providing insights into the internal regulatory processes involved in plant development. Much work remains to be done; however, this is a first step towards a new approach to the study of phenology that considers the causal relationship between external factors – both abiotic and biotic – and plant behaviour.

Acknowledgements

This study was funded by a NSERC Discovery Grant to Annie Deslauriers, the *Programme de Financement de la Recherche et Développement en Aménagement Forestier* (MFFP, Québec, Canada), Spruce Budworm Early Intervention Program of Natural Resources Canada and SERG-I. L. Balducci was funded by a MITACS Accelerate Fellowship in collaboration with SOPFIM. The work of F. Cartenì was funded by the project AIM1850344 of the AIM (Attraction and International Mobility) Program, financed by the Italian Ministry of Education, University and Research (MIUR). We thank Rémi Saint-Amant and Jacques Régnière for their helpful comments.

Competing interests



None declared.

Author contributions

FC, ADeslauriers and SM conceived and designed the study. FC and SM conceived and implemented the model. FC, ES and VN performed the analyses. FC, LB and ADeslauriers wrote the manuscript. ADeslauriers, LB and ADupont provided data. All authors contributed to the article and approved the submitted version.

ORCID

Lorena Balducci  <https://orcid.org/0000-0003-2261-943X>
Fabrizio Cartenì  <https://orcid.org/0000-0001-8985-1132>

Annie Deslauriers  <https://orcid.org/0000-0002-4994-5772>
Stefano Mazzoleni  <https://orcid.org/0000-0002-1132-2625>

Data availability

Sugar and phenological datasets for the Canadian experiments are available at doi: [10.5683/SP3/MVRZMQ](https://doi.org/10.5683/SP3/MVRZMQ). Data for the SPRUCE experiment can be found at: <https://mnspruce.ornl.gov/datasets/public>.

References

- Adams HD, Germino MJ, Breshears DD, Barron-Gafford GA, Guardiola-Claramonte M, Zou CB, Huxman TE. 2013. Nonstructural leaf carbohydrate dynamics of *Pinus edulis* during drought-induced tree mortality reveal role for carbon metabolism in mortality mechanism. *New Phytologist* 197: 1142–1151.
- Ainsworth EA, Bush DR. 2011. Carbohydrate export from the leaf: a highly regulated process and target to enhance photosynthesis and productivity. *Plant Physiology* 155: 64–69.
- Antonucci S, Rossi S, Deslauriers A, Lombardi F, Marchetti M, Tognetti R. 2015. Synchronisms and correlations of spring phenology between apical and lateral meristems in two boreal conifers. *Tree Physiology* 35: 1086–1094.
- Badeck FW, Bondeau A, Böttcher K, Doktor D, Lucht W, Schaber J, Sitch S. 2004. Response of spring phenology to climate change. *New Phytologist* 162: 265–309.
- Barbier FF, Lunn JE, Beveridge CA. 2015. Ready, steady, go! A sugar hit starts the race to shoot branching. *Current Opinion in Plant Biology* 25: 39–45.
- Basler D. 2016. Evaluating phenological models for the prediction of leaf-out dates in six temperate tree species across central Europe. *Agricultural and Forest Meteorology* 217: 10–21.
- Battaglia M, Pinkard EA, Sands PJ, Bruce JL, Quentin A. 2011. Modelling the impact of defoliation and leaf damage on forest plantation function and production. *Ecological Modelling* 222: 3193–3202.
- Beil I, Kreyling J, Meyer C, Lemcke N, Malyshev AV. 2021. Late to bed, late to rise – warmer autumn temperatures delay spring phenology by delaying dormancy. *Global Change Biology* 27: 5806–5817.
- Bellemin-Noël B, Bourassa S, Despland E, De Grandpré L, Pureswaran DS. 2021. Improved performance of the eastern spruce budworm on black spruce as warming temperatures disrupt phenological defences. *Global Change Biology* 27: 3358–3366.
- Bigras FJ, Bertrand A. 2006. Responses of *Picea mariana* to elevated CO₂ concentration during growth, cold hardening and dehardening: phenology, cold tolerance, photosynthesis and growth. *Tree Physiology* 26: 875–888.
- Bigras FJ, Ryppö A, Lindström A, Stattin E. 2001. Cold acclimation and deacclimation of shoots and roots of conifer seedlings. In: Bigras FJ, Colombo SJ, eds. *Conifer cold hardiness*. Dordrecht, the Netherlands: Springer, 57–88.
- Bonser SP, Aarssen LW. 2003. Allometry and development in herbaceous plants: functional responses of meristem allocation to light and nutrient availability. *American Journal of Botany* 90: 404–412.
- Bouchard M, Pernot C. 2021. Climate and size of previous cone crops contribute to large-scale synchronous cone production in balsam fir. *Canadian Journal of Forest Research* 51: 638–646.
- Caffarra A, Donnelly A, Chuine I. 2011. Modelling the timing of *Betula pubescens* budburst. II. Integrating complex effects of photoperiod into process-based models. *Climate Research* 46: 159–170.
- Cannell MGR, Smith RI. 1983. Thermal time, chill days and prediction of budburst in *Picea sitchensis*. *Journal of Applied Ecology* 20: 951–963.
- Celedon JM, Bohlmann J. 2019. Oleoresin defenses in conifers: chemical diversity, terpene synthases and limitations of oleoresin defense under climate change. *New Phytologist* 224: 1444–1463.
- Chomba BM, Guy RD, Weger HG. 1993. Carbohydrate reserve accumulation and depletion in Engelmann spruce (*Picea engelmannii* Parry): effects of cold storage and pre-storage CO₂ enrichment. *Tree Physiology* 13: 351–364.

- Chuine I. 2000. A unified model for budburst of trees. *Journal of Theoretical Biology* 207: 337–347.
- Chuine I. 2010. Why does phenology drive species distribution? *Philosophical Transactions of the Royal Society of London. Series B: Biological Sciences* 365: 3149–3160.
- Chuine I, Beaubien EG. 2001. Phenology is a major determinant of tree species range. *Ecology Letters* 4: 500–510.
- Cook BI, Wolkovich EM, Davies TJ, Ault TR, Betancourt JL, Allen JM, Bolmgren K, Cleland EE, Crimmins TM, Kraft NJB *et al.* 2012. Sensitivity of spring phenology to warming across temporal and spatial climate gradients in two independent databases. *Ecosystems* 15: 1283–1294.
- Cooke JE, Eriksson ME, Junttila O. 2012. The dynamic nature of bud dormancy in trees: environmental control and molecular mechanisms. *Plant, Cell & Environment* 35: 1707–1728.
- Damascos MA, Prado CHBA, Ronquim CC. 2005. Bud composition, branching patterns and leaf phenology in cerrado woody species. *Annals of Botany* 96: 1075–1084.
- De Barba D, Rossi S, Deslauriers A, Morin H. 2016. Effects of soil warming and nitrogen foliar applications on bud burst of black spruce. *Trees – Structure and Function* 30: 87–97.
- Decourteix M, Alves G, Bonhomme M, Peuch M, Ben Baaziz K, Brunel N, Guilliot A, Rageau R, Ameglio T, Petel G *et al.* 2008. Sucrose (JrSUT1) and hexose (JrHT1 and JrHT2) transporters in walnut xylem parenchyma cells: their potential role in early events of growth resumption. *Tree Physiology* 28: 215–224.
- De Grandpré L, Marchand M, Kneeshaw DD, Paré D, Boucher D, Bourassa S, Gervais D, Simard M, Griffin JM, Pureswaran DS. 2022. Defoliation-induced changes in foliage quality may trigger broad-scale insect outbreaks. *Communications Biology* 5: 463.
- Delpierre N, Vitasse Y, Chuine I, Guillemot J, Bazot S, Rutishauser T, Rathgeber CBK. 2016. Temperate and boreal forest tree phenology: from organ-scale processes to terrestrial ecosystem models. *Annals of Forest Science* 73: 5–25.
- Deslauriers A, Beaulieu M, Balducci L, Giovannelli A, Gagnon M-J, Rossi S. 2014. Impact of warming and drought on carbon balance related to wood formation in black spruce. *Annals of Botany* 114: 335–345.
- Deslauriers A, Caron L, Rossi S. 2015. Carbon allocation during defoliation: testing a defense-growth trade-off in balsam fir. *Frontiers in Plant Science* 6: 00338.
- Deslauriers A, Fournier M-P, Carteni F, Mackay J. 2019. Phenological shifts in conifer species stressed by spruce budworm defoliation. *Tree Physiology* 39: 590–605.
- Deslauriers A, Garcia L, Charrier G, Buttò V, Pichette A, Paré M. 2021. Cold acclimation and deacclimation in wild blueberry: direct and indirect influence of environmental factors and non-structural carbohydrates. *Agricultural and Forest Meteorology* 301–302: 108349.
- Farquhar GD, von Caemmerer S, Berry JA. 1980. A biochemical model of photosynthetic CO₂ assimilation in leaves of C₃ species. *Planta* 149: 78–90.
- Fournier M-P, Paré MC, Buttò V, Delagrangé S, Lafond J, Deslauriers A. 2020. How plant allometry influences bud phenology and fruit yield in two *Vaccinium* species. *Annals of Botany* 126: 825–835.
- González-González BD, García-González I, Vázquez-Ruiz RA. 2013. Comparative cambial dynamics and phenology of *Quercus robur* L. and *Q. pyrenaica* Willd. in an Atlantic forest of the northwestern Iberian Peninsula. *Trees* 27: 1571–1585.
- Gray DR. 2008. The relationship between climate and outbreak characteristics of the spruce budworm in eastern Canada. *Climatic Change* 87: 361–383.
- Guak S, Olszyk DM, Fuchigami LH, Tingey DT. 1998. Effects of elevated CO₂ and temperature on cold hardiness and spring bud burst and growth in Douglas-fir (*Pseudotsuga menziesii*). *Tree Physiology* 18: 671–679.
- Hamann E, Blevins C, Franks SJ, Jameel MI, Anderson JT. 2021. Climate change alters plant–herbivore interactions. *New Phytologist* 229: 1894–1910.
- Hänninen H. 1990. Modelling bud dormancy release in trees from cool and temperate regions. *Acta Forestalia Fennica* 213: 1–47.
- Hanson PJ, Riggs JS, Nettles WR, Phillips JR, Krassovski MB, Hook LA, Gu L, Richardson AD, Aubrecht DM, Ricciuto DM *et al.* 2017. Attaining whole-ecosystem warming using air and deep-soil heating methods with an elevated CO₂ atmosphere. *Biogeosciences* 14: 861–883.
- Huang JG, Deslauriers A, Rossi S. 2014. Xylem formation can be modeled statistically as a function of primary growth and cambium activity. *New Phytologist* 203: 831–841.
- Iqbal N, Masood A, Khan N. 2012. Analyzing the significance of defoliation in growth, photosynthetic compensation and source-sink relations. *Photosynthetica* 50: 161–170.
- Jach ME, Ceulemans R. 1999. Effects of elevated atmospheric CO₂ on phenology, growth and crown structure of Scots pine (*Pinus sylvestris*) seedlings after two years of exposure in the field. *Tree Physiology* 19: 289–300.
- Johnsen KH, Seiler JR. 1996. Growth, shoot phenology and physiology of diverse seed sources of black spruce: I. Seedling responses to varied atmospheric CO₂ concentrations and photoperiods. *Tree Physiology* 16: 367–373.
- Klein T, Vitasse Y, Hoch G. 2016. Coordination between growth, phenology and carbon storage in three coexisting deciduous tree species in a temperate forest. *Tree Physiology* 36: 847–855.
- Koch K. 2004. Sucrose metabolism: regulatory mechanisms and pivotal roles in sugar sensing and plant development. *Plant Biology* 7: 235–246.
- Laitat E, Loosveldt P, Boussard H, Hirvijarvi E. 1994. Study on major morphological, physiological and biochemical processes likely to be affected under combined effects of increasing atmospheric CO₂ concentrations and elevated temperature in partial ecosystem enclosures. In: Veroustraete F, Ceulemans R, eds. *Vegetation, modeling and climatic change effects*. The Hague, the Netherlands: Academic Press, 37–52.
- Lauder JD, Moran EV, Hart SC. 2019. Fight or flight? Potential tradeoffs between drought defense and reproduction in conifers. *Tree Physiology* 39: 1071–1085.
- Le Roncé I, Toïgo M, Dardevet E, Venner S, Limousin J-M, Chuine I. 2020. Resource manipulation through experimental defoliation has legacy effects on allocation to reproductive and vegetative organs in *Quercus ilex*. *Annals of Botany* 126: 1165–1179.
- Lieth H. 1974. *Phenology and seasonality modelling*. Berlin, Germany: Springer, XV, 444.
- Liu Q, Fu YH, Zhu Z, Liu Y, Liu Z, Huang M, Janssens IA, Piao S. 2016. Delayed autumn phenology in the Northern Hemisphere is related to change in both climate and spring phenology. *Global Change Biology* 22: 3702–3711.
- Lunn JE, Feil R, Hendriks JH, Gibon Y, Morcuende R, Osuna D, Scheible W-R, Carillo P, Hajirezaei M-R, Stitt M. 2006. Sugar-induced increases in trehalose 6-phosphate are correlated with redox activation of ADP-glucose pyrophosphorylase and higher rates of starch synthesis in *Arabidopsis thaliana*. *Biochemical Journal* 397: 139–148.
- Man R, Lu P, Dang Q-L. 2017. Cold hardiness of white spruce, black spruce, jack pine, and lodgepole pine needles during dehardening. *Canadian Journal of Forest Research* 47: 1116–1122.
- Mason MG, Ross JJ, Babst BA, Wienclaw BN, Beveridge CA. 2014. Sugar demand, not auxin, is the initial regulator of apical dominance. *Proceedings of the National Academy of Sciences, USA* 111: 6092–6097.
- Meng P, Bai X, Li H, Song X, Zhang X. 2015. Cold hardiness estimation of *Pinus densiflora* var. *zhangwuensis* based on changes in ionic leakage, chlorophyll fluorescence and other physiological activities under cold stress. *Journal of Forestry Research* 26: 641–649.
- Menzel A, Sparks TH, Estrella N, Koch E, Aasa A, Ahas R, Alm-Kübler K, Bissolli P, Braslavská O, Briede A *et al.* 2006. European phenological response to climate change matches the warming pattern. *Global Change Biology* 12: 1969–1976.
- Millard P, Hester A, Wendler R, Baillie G. 2001. Interspecific defoliation responses of trees depend on sites of winter nitrogen storage. *Functional Ecology* 15: 535–543.
- Murray MB, Ceulemans R. 1998. Will tree foliage be larger and live longer? In: Jarvis PG, ed. *European forests and global change. The likely impacts of rising CO₂ and temperature*. Cambridge, UK: Cambridge University Press, 94–125.
- Murray MB, Smith RI, Leith ID, Fowler D, Lee HSJ, Friend AD, Jarvis PG. 1994. Effects of elevated CO₂, nutrition and climatic warming on bud phenology in Sitka spruce (*Picea sitchensis*) and their impact on the risk of frost damage. *Tree Physiology* 14: 691–706.
- Niinemets Ü, Valladares F. 2004. Photosynthetic acclimation to simultaneous and interacting environmental stresses along natural light gradients: optimality and constraints. *Plant Biology* 6: 254–268.

- Park J-Y, Canam T, Kang K-Y, Unda F, Mansfield SD. 2009. Sucrose phosphate synthase expression influences poplar phenology. *Tree Physiology* 29: 937–946.
- Piao S, Liu Q, Chen A, Janssens IA, Fu Y, Dai J, Liu L, Lian X, Shen M, Zhu X. 2019. Plant phenology and global climate change: current progresses and challenges. *Global Change Biology* 25: 1922–1940.
- Piao S, Tan J, Chen A, Fu YH, Ciais P, Liu Q, Janssens IA, Vicca S, Zeng Z, Jeong S-J *et al.* 2015. Leaf onset in the northern hemisphere triggered by daytime temperature. *Nature Communications* 6: 6911.
- Piene H. 1989. Spruce budworm defoliation and growth loss in young balsam fir: defoliation in spaced and unspaced stands and individual tree survival. *Canadian Journal of Forest Research* 19: 1211–1217.
- Pureswaran DS, Neau M, Marchand M, De Grandpré L, Kneeshaw D. 2019. Phenological synchrony between eastern spruce budworm and its host trees increases with warmer temperatures in the boreal forest. *Ecology and Evolution* 9: 576–586.
- Quiring D, McKinnon M. 1999. Why does early-season herbivory affect subsequent budburst? *Ecology* 80: 1724–1735.
- Régnière J, Saint-Amant R, Béchard A, Moutaoufik A. 2017. *BioSIM 11 – user's manual*. Quebec, QC, Canada: Canadian Forest Service.
- Reich PB, Sendall KM, Stefanski A, Rich RL, Hobbie SE, Montgomery RA. 2018. Effects of climate warming on photosynthesis in boreal tree species depend on soil moisture. *Nature* 562: 263–267.
- Ren P, Néron V, Rossi S, Liang E, Bouchard M, Deslauriers A. 2020. Warming counteracts defoliation-induced mismatch by increasing herbivore–plant phenological synchrony. *Global Change Biology* 26: 2072–2080.
- Repo T, Hänninen H, Kellomäki S. 1996. The effects of long-term elevation of air temperature and CO₂ on the frost hardiness of Scots pine. *Plant, Cell & Environment* 19: 209–216.
- Richardson AD, Latimer JM, Nettles WR, Heiderman RR, Warren JM, Hanson PJ. 2018. *SPRUCES ground observations of phenology in experimental plots, 2016–2017*. Oak Ridge, TN, USA: Oak Ridge National Laboratory, TES SFA, US Department of Energy. doi: [10.3334/CDIAC/spruce.044](https://doi.org/10.3334/CDIAC/spruce.044).
- Rook DA. 1985. Physiological constraints on yield. In: Tigerstedt PMA, Puttonen P, Roski V, eds. *Crop physiology of forest trees*. Helsinki, Finland: Helsinki University Press, 1–19.
- Rossi S, Isabel N. 2017. The timing of bud break in warming conditions: variation among seven sympatric conifer species from Eastern Canada. *International Journal of Biometeorology* 61: 1983–1991.
- Sarvas R. 1974. Investigations on the annual cycle of development of forest trees: II. Autumn dormancy and winter dormancy. *Communications Instituti Forestalis Fenniae* 84: 101.
- Schaberg PG, Snyder MC, Shane JB, Donnelly JR. 2000. Seasonal patterns of carbohydrate reserves in red spruce seedlings. *Tree Physiology* 20: 549–555.
- Schädel C, Nettles WR, Heiderman RR, Pearson KJ, Richardson AD, Hanson PJ. 2019. *SPRUCES ground observations of phenology in experimental plots 2018*. Oak Ridge, TN, USA: Oak Ridge National Laboratory, TES SFA, US Department of Energy. doi: [10.25581/spruce.073/1557731](https://doi.org/10.25581/spruce.073/1557731).
- Schädel C, Pearson KJ, Nettles WR, Richardson AD, Hanson PJ. 2020. *SPRUCES ground observations of phenology in experimental plots 2019*. Oak Ridge, TN, USA: Oak Ridge National Laboratory, TES SFA, US Department of Energy. doi: [10.25581/spruce.087/1693415](https://doi.org/10.25581/spruce.087/1693415).
- Schädel C, Pearson KJ, Richardson AD, Warren JM, Hanson PJ. 2021. *SPRUCES ground observations of phenology in experimental plots 2020*. Oak Ridge, TN, USA: Oak Ridge National Laboratory, TES SFA, US Department of Energy. doi: [10.25581/spruce.094/1824175](https://doi.org/10.25581/spruce.094/1824175).
- Schoonmaker AL, Hillbrand RM, Lieffers VJ, Chow PS, Landhäusser SM. 2021. Seasonal dynamics of non-structural carbon pools and their relationship to growth in two boreal conifer tree species. *Tree Physiology* 41: 1563–1582.
- Seiwa K. 1999. Changes in leaf phenology are dependent on tree height in *Acer mono*, a deciduous broad-leaved tree. *Annals of Botany* 83: 355–361.
- Shampine LF, Reichelt MW. 1997. The MATLAB ODE suite. *SIAM Journal on Scientific Computing* 18: s1064827594276424.
- Signarbieux C, Toledano E, Sanginés de Carcer P, Fu YH, Schlaepfer R, Buttler A, Vitisse Y. 2017. Asymmetric effects of cooler and warmer winters on beech phenology last beyond spring. *Global Change Biology* 23: 4569–4580.
- Singh RK, Svystun T, Aldahmash B, Jönsson AM, Bhalerao RP. 2017. Photoperiod- and temperature-mediated control of phenology in trees – a molecular perspective. *New Phytologist* 213: 511–524.
- Smith NG, Dukes JS. 2013. Plant respiration and photosynthesis in global-scale models: incorporating acclimation to temperature and CO₂. *Global Change Biology* 19: 45–63.
- Stitt M, Zeeman SC. 2012. Starch turnover: pathways, regulation and role in growth. *Plant Biology* 15: 282–292.
- Strimbeck GR, Schaberg PG, Fossdal CG, Schröder WP, Kjellsen TD. 2015. Extreme low temperature tolerance in woody plants. *Frontiers in Plant Science* 6: 884.
- Svobodová H, Lipavská H, Albrechtová J. 2000. Non-structural carbohydrate status in Norway spruce buds in the context of annual bud structural development as affected by acidic pollution. *Environmental and Experimental Botany* 43: 253–265.
- Taïbi K, Del Campo AD, Vilagrosa A, Bellés JM, López-Gresa MP, López-Nicolás JM, Mulet JM. 2018. Distinctive physiological and molecular responses to cold stress among cold-tolerant and cold-sensitive *Pinus halepensis* seed sources. *BMC Plant Biology* 18: 236.
- Tixier A, Gambetta GA, Godfrey J, Orozco J, Zwieniecki MA. 2019. Non-structural carbohydrates in dormant woody perennials; the tale of winter survival and spring arrival. *Frontiers in Forests and Global Change* 2: 18.
- Tjoelker MG, Oleksyn J, Reich PB. 1998. Temperature and ontogeny mediate growth response to elevated CO₂ in seedlings of five boreal tree species. *New Phytologist* 140: 197–210.
- Vitisse Y, Baumgarten F, Zohner CM, Kaewthongrach R, Fu YH, Walde MG, Moser B. 2021. Impact of microclimatic conditions and resource availability on spring and autumn phenology of temperate tree seedlings. *New Phytologist* 232: 537–550.
- Wang Y, Wu WH. 2017. Regulation of potassium transport and signaling in plants. *Current Opinion in Plant Biology* 39: 123–128.
- Wang H, Wu C, Ciais P, Peñuelas J, Dai J, Fu Y, Ge Q. 2020. Overestimation of the effect of climatic warming on spring phenology due to misrepresentation of chilling. *Nature Communications* 11: 4945.
- Way DA, Sage RF. 2008. Thermal acclimation of photosynthesis in black spruce [*Picea mariana* (Mill.) B.S.P.]. *Plant, Cell & Environment* 31: 1250–1262.
- Woodruff DR, Meinzer FC. 2011. Water stress, shoot growth and storage of non-structural carbohydrates along a tree height gradient in a tall conifer. *Plant, Cell & Environment* 34: 1920–1930.
- Zani D, Crowther Thomas W, Mo L, Renner Susanne S, Zohner CM. 2020. Increased growing-season productivity drives earlier autumn leaf senescence in temperate trees. *Science* 370: 1066–1071.
- Zwieniecki MA, Tixier A, Sperling O. 2015. Temperature-assisted redistribution of carbohydrates in trees. *American Journal of Botany* 102: 1216–1218.

Supporting Information

Additional Supporting Information may be found online in the Supporting Information section at the end of the article.

Fig. S1 Response functions of the main model processes to temperature.

Fig. S2 Summary of the dataset and measurements used for model calibration and validation.

Fig. S3 Allometric relations between branch length and dry weight for black spruce, white spruce and balsam fir.

Fig. S4 Comparison of simulated budbreak dates when using data from the *in situ* weather station at the Mont-Valin site (Gaspard, SLSJ) or BioSIM v.1.1, used to extract the local climate.

Fig. S5 Model simulations of *Picea glauca* and *Abies balsamea* grown during the glasshouse experiment.

Fig. S6 Results of the GDD model calibration and validation.

Methods S1 Details on the model equations, experimental plots and data collection.

Methods S2 Details on the GDD model implementation, calibration and validation.

Table S1 Calculated variables used in the model equations.

Table S2 Initial values of state variables, model inputs and fixed parameters.

Table S3 Model calibrated parameters with description and simulation values.

Table S4 Characteristics of the experimental plots distributed within three regions in Québec (Canada) and one in Minnesota (USA).

Table S5 Number of data points per observed output for each species in the two calibration procedures.

Table S6 Results of the two-way ANOVA with DOY as dependent variable and elevated CO₂ and temperature treatments as independent variables.

Table S7 Results of the GLM with DOY as response variable and CO₂ (+0 and +500 ppm) and temperature (+0°C, +2.25°C, +4.5°C, +6.75°C and +9°C) treatments as categorical predictors.

Please note: Wiley is not responsible for the content or functionality of any Supporting Information supplied by the authors. Any queries (other than missing material) should be directed to the *New Phytologist* Central Office.